Automatic Cluster Detection in Hyperspectral Images using Quantum Walrus Optimizers

Tulika Dutta[1,*,†], Siddhartha Bhattacharyya[2,†], Bijaya Ketan Panigrahi[3,†], Jan Platos[4,†], Ivan Zelinka[5,†] and Vaclav Snasel[6,†]

[1]*Department of Electrical Engineering, IIT Delhi, New Delhi, India, and Department of Information Technology, Manipal Institute of Technology Bengaluru, Manipal Academy of Higher Education, Manipal, India*
[2]*VSB Technical University of Ostrava, Ostrava, Czech Republic*
[3]*Department of Electrical Engineering, IIT Delhi, New Delhi, India*
[4]*VSB Technical University of Ostrava, Ostrava, Czech Republic*
[5]*VSB Technical University of Ostrava, Ostrava, Czech Republic*
[6]*VSB Technical University of Ostrava, Ostrava, Czech Republic*

Abstract

The task of determining the correct number of clusters in hyperspectral images is not a straightforward procedure as the images feature complex spectral data, redundancy, and lack of validation images. Hence, automatic clustering methods are often preferred in practical applications, as they can effectively handle the complexity of spectral data and the absence of validation images. This study introduces two novel algorithms viz., the *Qubit* Walrus Optimizer (QbWaO) and *Qutrit* Walrus Optimizer (QtWaO) to leverage quantum principles to address the limitations of classical optimization techniques, which are inspired by the breeding behavior of walruses. QbWaO and QtWaO are designed to automatically detect clusters in hyperspectral images (HSI) by effectively balancing exploration and exploitation. This makes them particularly suited for high-dimensional clustering tasks in a real time environment. The concept of quantum Hadamard gates is used to initialize the population and induce diversity. The optimal clusters are then determined using the Adjusted Rand Index as the fitness function. F score and the F' score are used to determine the quality of the grouping. The comparative results suggest that the proposed methods outperform classical approaches in most scenarios, demonstrating their effectiveness in automatically clustering hyperspectral images.

Keywords

walrus optimizer, qutrit, qubit, Hadamard gate, hyperspectral image

1. Introduction

The emergence of spectral cameras and sensors has significantly improved the ability to collect detailed information about ground data in various fields, such as agriculture, law enforcement, geography, and military applications [1]. Hyperspectral sensors capture data across hundreds of contiguous spectral bands. This broader spectral and wide area coverage helps represent a combination of multiple materials, each contributing to the pixel's overall spectral signature with varying abundance levels. Hyperspectral imaging (HSI) is a powerful technology, but the vast amount of data in contiguous spectral bands presents a major computational challenge. Band Selection (BS) techniques are commonly employed as a preprocessing step to identify unique spectral bands. A key challenge is designing effective criteria for informative bands while retaining important spectral information. Recently, information theory-based methods [1] have demonstrated great potential in HSI band selection.

The 2024 Sixth Doctoral Symposium on Intelligence Enabled Research (DoSIER 2024), November 28–29, 2024, Jalpaiguri, India
*Corresponding author.
†These authors contributed equally.
munai.tulika@gmail.com (T. Dutta); dr.siddhartha.bhattacharyya@gmail.com (S. Bhattacharyya); bijayaketanpanigrahi@gmail.com (B. K. Panigrahi); jan.platos@vsb.cz (J. Platos); ivan.zelinka@vsb.cz (I. Zelinka); vaclav.snasel@vsb.cz (V. Snasel)
0000-0003-2672-5360 (T. Dutta); 0000-0001-7296-7999 (S. Bhattacharyya); 0000-0003-2062-2889 (B. K. Panigrahi); 0000-0002-8481-0136 (J. Platos); 0000-0002-3858-7340 (I. Zelinka); 0000-0002-5213-3302 (V. Snasel)

One critical task in HSI processing is automatic cluster detection [2]. This aims to identify underlying patterns, classes, or regions without ground-truth images. Traditional clustering algorithms, such as k-means [3] or fuzzy c-means [4], often struggle with HSI's high-dimensional, nonlinear nature. Optimization-based clustering techniques have gained popularity to overcome these challenges. Nature-inspired metaheuristic optimization techniques, such as Genetic Algorithms [5], Particle Swarm Optimization [6], and Tabu Search [7], have emerged as powerful tools in HSI clustering. These methods effectively explore the vast solution space, adapt to HSI data's complex spectral signatures and high-dimensional structure, and avoid local minima, thus offering superior performance over traditional clustering algorithms. The Walrus Optimizer (WaO) [8] is a relatively new optimization algorithm offering efficient global search capability while balancing navigating and leveraging the search space. WaO [8] can suffer from slow and premature convergence when solving complex problems.
The No Free Lunch Theorem affirms that no one-size-fits-all algorithm can effectively address all NP-hard problems [9]. Researchers are creating improved metaheuristic algorithms to effectively address the diverse array of real-world challenges. In recent years, quantum-based metaheuristic methods have transpired as potential solutions to these problems [2]. These algorithms enhance search efficiency by employing quantum computing principles such as superposition and entanglement. In recent years, *qubit* or bi-level quantum metaheuristics have drawn substantial research attention, but developing higher-order quantum metaheuristics remains a complex challenge [10]. However, applying quantum-based approaches to complex clustering problems requires innovative designs and frameworks.
In this work, *qubit* and *qutrit* versions of the Walrus Optimizer algorithm viz., *Qubit* Walrus Optimizer (QbWaO) and the *Qutrit* Walrus Optimizer (QtWaO) are introduced. The breeding behavior of walruses has inspired these, and quantum principles have enhanced their limitations. QbWaO and QtWaO are designed to automatically detect clusters in hyperspectral images by leveraging quantum-inspired mechanisms to balance exploration and exploitation effectively. This makes it ideal for complex high-dimensional HSI clustering. Furthermore, QbWaO and QtWaO incorporate breeding-inspired dynamics and foraging behavior to maintain population diversity.
The primary contributions are as follows.

- emphQubit and *Qutrit*-Based WaO: This is the first instance of developing and applying multilevel quantum versions of the Walrus Optimizer Algorithm for clustering hyperspectral images.
- Enhanced Exploration Phase with Global Best Selection: Instead of selecting a random walrus, the global best solution or the best walrus is utilized during the exploration phase. This effectively guides the entire population towards the leader.
- Band Selection Based on Spectral Variability (BSSV) [11]: The proposed method selects the most dissimilar bands by utilizing spectral variability similarity, ensuring the removal of redundant information.
- Population Diversity Enhancement with *qubit* and *qutrit* Hadamard Gate: The population is initialized using either *qubit* or *qutrit* Hadamard gate, which equally distributes individuals across the search space, increasing diversity in the population.

The paper is organized as follows: Section 2 presents a brief review of the literature. Relevant concepts are discussed in Section 3. Section 4 contains the details of the main proposed work. Section 5 thoroughly describes the dataset used, the experimental design, and the result anyalysis. Finally, Section 6 offers a concise conclusion of the proposed methodology.

2. Brief Survey of Related Works

Hyperspectral imaging has revolutionized the way detail information about ground targets is captured and analyzed in various fields such as agriculture, geographical monitoring, and defense-based applications. However, this vast amount of data leads to significant computational challenges, necessitating effective band selection techniques to identify informative bands while preserving essential spectral information [11]. Recent studies have shown that information theory-based methods offer promising

results in HSI band selection, allowing for the extraction of critical features from complex datasets [1]. In [12], superpixel segmentation is performed to find the heterogeneous area in region-specific hypergraphs, and then a consensus matrix is built to select bands efficiently for hyperspectral imagery.
Clustering assessment metrics are employed to determine the optimal number of clusters. Adjusted Rand Index (*AIndex*) [13], and PBM index [14] are some well-known metrics.
Estimating optimal clusters in HSI is important as ground truth data is often absent [15]. A lot of HSI clustering methods have been reviewed in [15]. Although an effective process, unsupervised Artificial DNA Spectral Matching proposed in [16] takes a huge amount of time for execution. Optimization-based clustering techniques have gained traction in addressing these challenges. The Walrus Optimization Algorithm (WaO)[8] is a recent addition to this suite of optimization algorithms, distinguished by its efficient global search capabilities and its balanced approach to exploration and exploitation of the search space, but it suffers from slow and premature convergence. As no individual optimization algorithm can universally solve all NP-hard problems[9], developing enhanced metaheuristic algorithms that can adapt to a wide range of real-world challenges is needed.
In light of these considerations, quantum-based metaheuristic methods have emerged as potential solutions, harnessing the quantum computing principles, such as superposition, coherence and decoherence—to improve search efficiency [2]. While *qubit*-based quantum metaheuristics have garnered significant attention, advancing higher-order quantum metaheuristics, such as those utilizing *qutrits*, remains a complex challenge [10]. In [17], a *qubit*-based Grey Wolf Optimizer (QBGWO) is introduced, incorporating quantum rotation and NOT gates to enhance solution quality. A memetic quantum-inspired evolutionary algorithm was proposed in [18] which combines quantum genetic algorithms with tabu search. It balances global exploration via quantum rotation gates and local exploitation through directional mutations, achieving faster convergence and improved performance on benchmark functions. In [19], a *qubit* based Differential Evolution algorithm is developed for efficiently identifying optimal clusters without prior knowledge and outperforming competitive algorithms in accuracy and convergence speed.
While *qubit*-based algorithms generally outperform classical metaheuristics, they remain constrained by the No Free Lunch Theorem [9]. Consequently, there is significant research interest in developing higher-order quantum metaheuristics, specifically qudit-based methods. A three-valued quantum or (qutrit) based Genetic Algorithm was developed in [20]. In [2], the Differential Evolution algorithm has been introduced for the automated clustering of hyperspectral images. Additionally, six quantum methodologies based on the Artificial Hummingbird Algorithm, Particle Swarm Optimization, and Genetic Algorithms have been presented in [10], utilizing both bi-level and tri-level quantum logic for unsupervised clustering of HSI data.

3. Significant Related Concepts

This section discusses several key concepts, viz., band selection method used, foundational principles of quantum computing, and the WaO[8] algorithm.

3.1. Band Selection Based on Spectral Variability [11]

Spectral Information Divergence (SID) measures the difference between two spectral bands by evaluating their probability distributions. To compute the SID first, the probability vectors are defined as follows. For two spectral bands SVB_j and SVB_k, we first define their probability vectors as
- For band SVB_i:

$$Pa_i = \frac{SVB_{ji}}{\sum_{k=1}^{Ba} SVB_{jL}}, \quad i = 1, 2, \ldots, Ba$$

- For band SVB_j:

$$Pa_j = \frac{SVB_{ki}}{\sum_{k=1}^{Ba} SVB_{jk}}, \quad i = 1, 2, \ldots, Ba$$

where, Ba is the spectral dimension of the HSI dataset. The SID between the two bands SVB_i and SVB_j are defined using the Kullback-Leibler divergence (relative entropy) as

$$SID(SVB_i, SVB_j) = RE(SVB_i||SVB_j) + RE(SVB_j||SVB_i), \tag{1}$$

where, the Kullback-Leibler divergence $RE(SVB_i||SVB_j)$ is given by

$$RE(SVB_i||SVB_j) = \sum_{k=1}^{Ba} Pa_{ik} \log \frac{Pa_{ik}}{Pa_{jk}}. \tag{2}$$

The channel transition probability is defined as

$$BSSV_{j|i} = \frac{SID(SVB_i, SVB_j)}{\sum_{l=1}^{Ba} SID(SVB_l, SVB_j)}, \tag{3}$$

The bands with the lowest SID values are selected as the distinct bands because they exhibit the least similarity in spectral information.

3.2. Quantum Computing Principles

Quantum-based machines represent a powerful computational paradigm that merges quantum mechanics with fundamentals of computing [10]. The basic unit of quantum machines are the *qubit*. *Qubits* exist in two distinct states: $|0\rangle$ and $|1\rangle$ [10]. These states can be expressed mathematically in the following column vector notation [21].

$$|0\rangle = \begin{pmatrix} 1 \\ 0 \end{pmatrix}, \quad |1\rangle = \begin{pmatrix} 0 \\ 1 \end{pmatrix} \tag{1}$$

Qubits exist in a superposition of its basis states ($|0\rangle$ and $|1\rangle$). The number of states that can be represented by n *qubits* in superposition grows exponentially (2^n) and thus provides increased computational efficacy with fewer resources. The superposition state of a *qubit*, denoted as $|S_t\rangle$ (where $t = 2$ for *qubit*), is given by

$$|S_t\rangle = s_0|0\rangle + s_1|1\rangle \tag{2}$$

The probabilities that the *qubits* are in states $|0\rangle$ or $|1\rangle$ are represented by the complex coefficients s_0 and s_1, respectively. These probabilities also satisfy the following condition.

$$0 \leqslant |s_t|^2 \leqslant 1, \quad \text{for } t = 0, 1 \tag{3}$$

The normalization condition for a *qubit* is expressed as follows [21].

$$s_0^2 + s_1^2 = 1 \tag{4}$$

Quantum systems can exhibit a wider range of discrete energy levels and exist in more than two states, known as *qudits* [2]. The smallest multilevel quantum system is called a *qutrit* [2]. A *qutrit* can similarly be represented as

$$|0\rangle = \begin{pmatrix} 1 \\ 0 \\ 0 \end{pmatrix}, \quad |1\rangle = \begin{pmatrix} 0 \\ 1 \\ 0 \end{pmatrix}, \quad |2\rangle = \begin{pmatrix} 0 \\ 0 \\ 1 \end{pmatrix} \tag{5}$$

Qudits offer better performance than *qubits* [10]. They require fewer units to achieve superior results than a larger number of *qubits*, thus reducing computation time. Mathematically, to represent the same information as n *qubits*, only $\frac{n}{\log_2(3)}$ *qutrits* are needed, resulting in an efficiency increase of approximately $\log_2(3) \approx 1.6$ [2]. This reduction significantly lowers decoherence in *qudit*-based systems, enhancing their computational power. A *qutrit* can be expressed in a superposition state as follows.

$$|S_t\rangle = s_0|0\rangle + s_1|1\rangle + s_2|2\rangle \tag{6}$$

The normalization condition for a *qutrit* is given by

$$s_0^2 + s_1^2 + s_2^2 = 1 \tag{7}$$

Furthermore, the probabilities associated with the states of a *qutrit* must satisfy the following condition.

$$0 \leqslant |s_t|^2 \leqslant 1, \quad \text{for } t = 0, 1, 2 \text{ (qutrit)} \tag{8}$$

3.3. Walrus Optimizer Algorithm [8]

The WaO [8] algorithm is based on the behavior of walruses. Their ways of migrating, breeding, roosting, and foraging are considered by Han et al.. This approach models walruses social structures and role divisions, assuming populations interpret behavior through danger and safety signals. The steps of WaO [8] are briefly described in Algorithm 1.
The WaO [8] uses a population of "walruses" (agents) to explore and exploit the search space for optimal solutions to optimization problems. The algorithm divides the population into adults (90%) and juveniles (10%), with different roles for males, females, and juveniles.
Key features of WaO [8] include danger and safety signals, which encompasses the phases of exploration and exploitation in the algorithm. In high-risk conditions, walruses migrate causing enhanced searching in the entire solution space, while in safer conditions, they reproduce causing exploitation of the search space. Migration is achieved by adjusting positions based on other walruses' locations, while reproduction involves updating positions through male influence (using a Halton sequence) and female influence from both the male and the best solution. Juveniles update their positions to avoid predators.

4. Proposed Work

The proposed methodology can be divided into two sections viz., *BSSV* based *Band Depletion* and Quantum Walrus Optimizer Algorithms. Band minimization is done as stated in Section 3.1.

4.1. Quantum Walrus Optimizers (QbWaO and QtWaO)

The *quantum* versions viz., *Qubit* Walrus Optimizer and *Qutrit* Walrus Optimizer algorithms follow the same steps as mentioned in Algorithm 1. The modifications introduced are as follows:

- *Qubit* or *Qutrit* Encoding and Observation [20] : The *qubit* walrus population is represented as follows.

$$\begin{bmatrix} s_{01} & s_{02} & s_{03} & \dots & s_{0n} \\ s_{11} & s_{12} & s_{13} & \dots & s_{1n} \end{bmatrix}$$

  Similarily, the *qutrit* walrus population is represented in the following manner.

$$\begin{bmatrix} s_{01} & s_{02} & s_{03} & \dots & s_{0n} \\ s_{11} & s_{12} & s_{13} & \dots & s_{1n} \\ s_{21} & s_{22} & s_{23} & \dots & s_{2n} \end{bmatrix}$$

  As Hadamard gate initializes all the states with equal amplitude values, *qubit* states are initialized in the following manner.

$$S_{n,d}^{It} = 1/sqrt(2) + 1/sqrt(2) \tag{23}$$

  where, $s_{01} = 1/sqrt(2)$ and $s_{11} = 1/sqrt(2)$ for each individual *qubit*. Similarly, the following method is used for a *qutrit*.

$$S_{n,d}^{It} = 1/sqrt(3) + 1/sqrt(3) + 1/sqrt(3) \tag{24}$$

Algorithm 1 Walrus Optimizer Algorithm [8]

Input: Population PoP consisting of n Walrus of d dimension, Maximum iterations MaT, rd_1, rd_2, rd_3,rd_4 and rd_5 are random numbers between (0,1), $MStep$ is Migration step, γ is a distress coefficient designated by random number between (0,1).
PoP is divided into 45% Male Walrus (MW) with top fitness values, 45% Female Walrus (FW) and 10% Young Walrus (YW) in Exploitation Phase. Best Male Walrus (BW1) has the highest fitness, and (BW2) has the second highest fitness value.
Initialize the population PoP using

$$PoP_{n,d} = \text{random}(0, 1) \tag{9}$$

Calculate fitness values F for each walrus
while $It \leq MaT$ **do**
    Calculate danger signal

$$Danger\ signal = D_{as} \cdot R \tag{10}$$

where, A, D_{as}, and R are given by

$$A = 1 - \frac{It}{MaT}, \quad D_{as} = 2 \times A, \quad R = 2 \times rd_1 - 1 \tag{11}$$

    if $|Danger\ signal| \geq 1$ **then**
        Exploration phase
        Update positions of each walrus

$$PoP_{n,d}^{It+1} = PoP_{n,d}^{It} + ms \tag{12}$$

where, the Migration step is calculated as

$$MStep = R_{n,d}^{It} - PoP_{n,d}^{It} \cdot b \cdot rd_3 \tag{13}$$

where, R is a randomly selected position, and

$$b = 1 - \frac{1}{1 + \exp\left(-\frac{It - MaT/2}{MaT \times 10}\right)} \tag{14}$$

    else
        Exploitation phase
        if Safety signal ≥ 0.5 **then**
            Breeding behavior
            for each MW **do**
                Use the Halton sequence to update the position
            end for
            for each FW **do**
                Update

$$\begin{aligned} FW_{n,d}^{\mathrm{It}+1} = FW_{n,d}^{\mathrm{It}} &+ a \cdot (MW_{n1,d1}^{\mathrm{It}} - FW_{n,d}^{\mathrm{It}}) \\ &+ (1 - A) \cdot (BW1_{d}^{\mathrm{It}} - FW_{n,d}^{\mathrm{It}}) \end{aligned} \tag{15}$$

            end for
            for each YW **do**
                Update position

$$YW_{n,d}^{It+1} = (P - YW_{n,d}^{It}) \cdot \gamma \tag{16}$$

where:

$$P = BW1_{d}^{It} + YW_{n,d}^{It} \cdot LP \tag{17}$$

LP is generated using Lévy distribution to imitate Lévy movement
            end for
        else
            Foraging behavior
            if $|Danger\ signal| \geq 0.5$ **then**
                Gathering behavior
                Update positions

$$PoP_{n,d}^{It+1} = \frac{BW1_{n,d}^{It} + BW2_{n,d}^{It}}{2} \tag{18}$$

where,

$$BW1_{n,d}^{It+1} = BW1_{n,d}^{It} - a_1 \cdot b_1 \cdot |BW1_{n,d}^{It} - PoP_{n,d}^{It}| \tag{19}$$

$$BW2_{n,d}^{It+1} = BW2_{n,d}^{It} - a_2 \cdot b_2 \cdot |BW2_{n,d}^{It} - PoP_{n,d}^{It}| \tag{20}$$

Calculate a and b

$$a_i = b \cdot rd_5 - b, \quad b_i = \tan(\theta), \quad i = 1, 2 \tag{21}$$

            else
                Fleeing behavior
                Update positions

$$PoP_{n,d}^{It+1} = PoP_{n,d}^{It} \cdot r - |BW1_{d} - PoP_{n,d}^{It}| \cdot rd_4 \tag{22}$$

            end if
        end if
    end if
    Update walrus positions
    Calculate fitness and update the best solution
    $It = It + 1$
end while
Output: The best solution

Algorithm 2 *Qubit* State Observation

for $i = 1$ **to** n **do**
  for $i = 1$ **to** d **do**
    $rand \leftarrow$ random number in range $[0, 1]$
    if $rand < s_{0_{n,d}}$ **then**
      $PoP_{n,d} \leftarrow 0$
    else
      $PoP_{n,d} \leftarrow 1$
    end if
  end for
end for

Algorithm 3 *Qutrit* State Observation

for $i = 1$ **to** n **do**
  for $i = 1$ **to** d **do**
    $rand \leftarrow$ random number in range $[0, 1]$
    if $rand < s_{0_{n,d}}$ **then**
      $PoP_{n,d} \leftarrow 0$
    else if $s_{0_{n,d}} \leq rand < s_{1_{n,d}}$ **then**
      $PoP_{n,d} \leftarrow 1$
    else
      $PoP_{n,d} \leftarrow 2$
    end if
  end for
end for

where, $s_{01} = 1/sqrt(3)$, $s_{11} = 1/sqrt(3)$ and $s_{21} = 1/sqrt(3)$. This ensures that the initial population is equally distributed in the solution space.
Equations (23) and (24) suffice the normalization principles stated in Section 3.2. The following Algorithms 2 and 3 are used for finding the probable classical state observations [20]. The notations of n, d and PoP are same as specified in Algorithm 1. The resulting classical representation in binary and ternary form after observations for each walrus are

$$\begin{bmatrix} 0 & 1 & 0 & 1 & 1 & 1 & 1 & 0 & 0 \cdots d \end{bmatrix} \tag{25}$$

$$\begin{bmatrix} 0 & 2 & 0 & 1 & 1 & 2 & 1 & 0 & 0 \cdots d \end{bmatrix} \tag{26}$$

- Equqation (13) is replaced by the equation given below.

$$MStep = BW_d^{It} - PoP_{n,d}^{It} \cdot b \cdot rd_3 \tag{27}$$

  Instead of considering any random Walrus, the best Walrus with the highest fitness value enhances the exploration phase.
- At the end of every iteration, it is checked whether the quantum normalization principles are adhered to. When it does not stand true Equations (23) and (24) are used to reinitialize those walruses.
- In every iteration, a random count of zeros is incorporated into the population for which PoP is true. The non-zero values designate the cluster centers using k-mean++ [3] algorithm, the appropriate clusters are constructed. The *AIndex* [13] is used as the Cluster Validity Index to identify the optimal cluster numbers.

The complexity of the band minimization is as follows:

$$O(m \times n \times d)$$

Table 1
Mean (Me), Standard Deviation (STD) and convergence time (CTime) for WaO [8], QbWaO, and QtWaO using AIndex [13] for WHU Dataset [22] [23]

No	Algorithm	Me	STD	Time
1	**WaO [8]**	0.4456	0.0594	974.3500
2	**QbWaO**	0.4737	0.0028	480.2580
3	**QtWaO**	0.4753	0.0034	**21.98680**

Here D bands are present each of dimensions $M \times N$ pixels. For the QbWaO, if P is a randomly chosen pixel intensity value, d represnts the length of individual population, MaT is the total number of iterations then the worst-case time complexity is:

$$O(2 \times P \times d \times MaT)$$

For QtWaO, the time complexity is as follows:

$$O(3 \times P \times d \times MaT)$$

5. Findings and Analysis

This section presents the various parameters used, the dataset employed, the statistical tests conducted, and the analysis of the experimental results.

5.1. HSI Dataset

The WHU-Hi-LongKou dataset (WHU) [22] [23] was collected in 2018, featuring scenes of Longkou Town in Hubei province, China. It has 9 classes spread over an agricultural landscape with six types of crops. It has a spatial dimension of 550 × 400 pixels and a spectral dimension of 270 spectral bands. The UAV-borne hyperspectral imagery has a spatial resolution of approximately 0.463 meters.

5.2. Experimental Configurations and Analysis

QbWaO and QtWaO are compared with their classical version WaO [8] using the WHU-Hi-LongKou dataset [22] [23]. To conduct an impartial study, all algorithms are executed for 50 times over 100 iterations. An Intel Core i7-8700 processor and a Windows 11 machine were used. All simulations were conducted on MATLAB 2023b. In WaO [8], each Walrus has dimensions of 20 and 20 walruses were considered. The dimensions were kept the same for both QbWaO and QtWaO. The number of walruses taken was 16 for QbWaO and 14 for QtWaO, respectively. For QbWaO, 8 male and female walruses and 2 young walruses were taken. In QtWaO, 7 male and female walruses and 2 young walruses were taken. The proposed methods are also compared with Kmeans [3] algorithm using taking the predefined cluster number as 6.
Various statistical tests like mean and standard deviation are recorded in Table 1 for all three algorithms. The time required for the convergence of each algorithm is noted in Table 1. From Table 1 and Figure 1 it can be observed that QtWaO takes far lesser time to converge than the other two algorithms.
Table 2 contains the optimal AIndex [13] values, automatically detected cluster numbers, F score [24] and F' score [24] are presented. The F score [24] and F' score [24] help determine the clustering quality. QtWaO produces 10 clusters nearest to the classes in the WHU Dataset [22] [23]. The clustered images, along with the minimized image produced by using BSSV [11] and the ground truth image of WHU Dataset [22] [23] are presented in Figure 2.
The null hypothesis is evaluated using the One-Way ANOVA test [25], which assesses whether the results originate from the same probability distribution. The null hypothesis is rejected if the p value is below the 1% significance level, indicating support for the alternative hypothesis. The results are

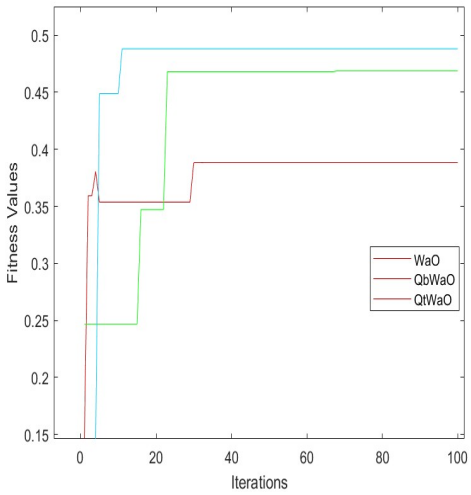

Figure 1: Convergence curve for WaO [8], QbWaO, and QtWaO results for WHU Dataset [22] [23]

Table 2
Optimal clusters detected (NC) and best fitness values using Adjusted Rand Index (*AIndex*) [13] and F and F' scores [24] for WaO [8], QbWaO, and QtWaO, evaluated on the WHU Dataset [22] [23]

No	Algorithm	AIndex [13]	NC	F Score	F' Score
1	**WaO [8]**	0.3883	4	0.3669	46.4787
2	**QbWaO**	0.4680	7	0.5492	68.5959
3	**QtWaO**	**0.4882**	**10**	**0.9467**	**84.1882**

Table 3
One-Way ANOVA Test [25] on WaO [8], QbWaO, and QtWaO results for WHU Dataset [22] [23]

Dataset	p-value	Significance
WHU Dataset [22] [23]	5.8623e-04	Highly Significant

summarized in Table 3. Additionally, Tukey's post hoc test [25] is conducted. The box plots for both tests are shown in Figure 3.

Based on the various tests conducted and the parameters evaluated, QtWaO generally outperforms QbWaO in most cases. Also, the population size and convergence speed of QtWaO are far better than those of both QbWaO and WaO.

6. Conclusion

Qubit and *Qutrit* Walrus Optimizer algorithms significantly advance unsupervised clustering for hyperspectral imagery. By integrating quantum principles and biological inspirations, QbWaO and QtWaO effectively address the challenges associated with the slow and premature convergence of the Walrus Optimizer algorithm. The enhanced exploration phase integrated with the Hadamard gate and band selection strategies improves clustering performance and ensures the robustness of the algorithms in high-dimensional spaces. The *qutrit* version performs better in almost all aspects, producing a near-optimal number of clusters in less time. Future work could explore enhancements to these quantum algorithms, including implementing more advanced quantum techniques and their application to various domains requiring sophisticated data clustering solutions. Additionally, parameter reduction can be implemented in the Walrus Optimizer.

Acknowledgments

Thanks to the developers of ACM consolidated LaTeX styles https://github.com/borisveytsman/acmart and to the developers of Elsevier updated LaTeX templates https://www.ctan.org/tex-archive/macros/latex/contrib/els-cas-templates.

Declaration on Generative AI

The author(s) have not employed any Generative AI tools.

References

[1] C.-I. Chang, Y.-M. Kuo, S. Chen, C.-C. Liang, K. Y. Ma, P. F. Hu, Self-mutual information-based band selection for hyperspectral image classification, IEEE Transactions on Geoscience and Remote Sensing 59 (2021) 5979–5997.

[2] T. Dutta, S. Bhattacharyya, B. K. Panigrahi, J. Platos, V. Snasel, Automatic hyperspectral image clustering using qutrit differential evolution, in: Y. Tan, Y. Shi (Eds.), Advances in Swarm Intelligence, Springer Nature Singapore, Singapore, 2024, pp. 280–294.

[3] D. Arthur, S. Vassilvitskii, k-means++: the advantages of careful seeding, in: Proceedings of the Eighteenth Annual ACM-SIAM Symposium on Discrete Algorithms, SODA '07, Society for Industrial and Applied Mathematics, USA, 2007, p. 1027–1035.

[4] J. C. Bezdek, R. Ehrlich, W. Full, FCM: The fuzzy c-means clustering algorithm, Computers & Geosciences 10 (1984) 191–203.

[5] J. Holland, Adaptation in natural and artificial systems: An introductory analysis with application to biology, control, and artificial intelligence, University of Michigan Press, 1975.

[6] Y. Shi, R. Eberhart, A modified particle swarm optimizer, in: 1998 IEEE International Conference on Evolutionary Computation Proceedings. IEEE World Congress on Computational Intelligence (Cat. No.98TH8360), 1998, pp. 69–73.

[7] F. Glover, M. Laguna, Tabu Search, Springer US, Boston, MA, 1998, pp. 2093–2229.

[8] M. Han, Z. Du, K. F. Yuen, H. Zhu, Y. Li, Q. Yuan, Walrus optimizer: A novel nature-inspired metaheuristic algorithm, Expert Systems with Applications 239 (2024) 122413.

[9] S. Mirjalili, S. M. Mirjalili, A. Lewis, Grey wolf optimizer, Advances in Engineering Software 69 (2014) 46–61.

[10] T. Dutta, S. Bhattacharyya, B. K. Panigrahi, I. Zelinka, L. Mrsic, Multi-level quantum inspired metaheuristics for automatic clustering of hyperspectral images, Quantum Machine Intelligence 5 (2023) 1–35.

[11] C.-I. Chang, An information-theoretic approach to spectral variability, similarity, and discrimination for hyperspectral image analysis, IEEE Transactions on Information Theory 46 (2000) 1927–1932.

[12] B. Fu, X. Sun, C. Cui, J. Zhang, X. Shang, Structure-preserved and weakly redundant band selection for hyperspectral imagery, IEEE Journal of Selected Topics in Applied Earth Observations and Remote Sensing 17 (2024) 12490–12504.

[13] S. Zhang, H.-S. Wong, Arimp: A generalized adjusted rand index for cluster ensembles, in: 2010 20th International Conference on Pattern Recognition, 2010, pp. 778–781.

[14] M. K. Pakhira, S. Bandyopadhyay, U. Maulik, Validity index for crisp and fuzzy clusters, Pattern recognition 37 (2004) 487–501.

[15] H. Zhai, H. Zhang, P. Li, L. Zhang, Hyperspectral image clustering: Current achievements and future lines, IEEE Geoscience and Remote Sensing Magazine 9 (2021) 35–67.

[16] H. Jiao, Y. Zhong, L. Zhang, An unsupervised spectral matching classifier based on artificial dna computing for hyperspectral remote sensing imagery, IEEE Transactions on Geoscience and Remote Sensing 52 (2014) 4524–4538.

[17] Y. Liu, C. Li, J. Xiao, Z. Li, W. Chen, X. Qu, J. Zhou, Qegwo: Energy-efficient clustering approach for industrial wireless sensor networks using quantum-related bioinspired optimization, IEEE Internet of Things Journal 9 (2022) 23691–23704.
[18] A. S. Hesar, M. Houshmand, A memetic quantum-inspired genetic algorithm based on tabu search, Evolutionary Intelligence 17 (2024) 1837–1853.
[19] A. Dey, S. Bhattacharyya, S. Dey, J. Platos, V. Snasel, A quantum inspired differential evolution algorithm for automatic clustering of real life datasets, Multimedia Tools and Applications 83 (2024) 8469–8498.
[20] V. Tkachuk, Quantum genetic algorithm based on qutrits and its application, Mathematical Problems in Engineering 2018 (2018) 8614073.
[21] T. Dutta, S. Bhattacharyya, S. Mukhopadhyay, Automatic clustering of hyperspectral images using qutrit exponential decomposition particle swarm optimization, in: 2021 IEEE International India Geoscience and Remote Sensing Symposium (InGARSS), 2021, pp. 289–292.
[22] Y. Zhong, X. Wang, Y. Xu, S. Wang, T. Jia, X. Hu, J. Zhao, L. Wei, L. Zhang, Mini-uav-borne hyperspectral remote sensing: From observation and processing to applications, IEEE Geoscience and Remote Sensing Magazine 6 (2018) 46–62.
[23] Y. Zhong, X. Hu, C. Luo, X. Wang, J. Zhao, L. Zhang, Whu-hi: Uav-borne hyperspectral with high spatial resolution (h2) benchmark datasets and classifier for precise crop identification based on deep convolutional neural network with crf, Remote Sensing of Environment 250 (2020) 112012.
[24] M. Borsotti, P. Campadelli, R. Schettini, Quantitative evaluation of color image segmentation results, Pattern Recognition Letters 19 (1998) 741–747.
[25] E. Liberto, D. Bressanello, G. Strocchi, C. Cordero, M. R. Ruosi, G. Pellegrino, C. Bicchi, B. Sgorbini, Hs-spme-ms-enose coupled with chemometrics as an analytical decision maker to predict in-cup coffee sensory quality in routine controls: Possibilities and limits, Molecules 24 (2019).

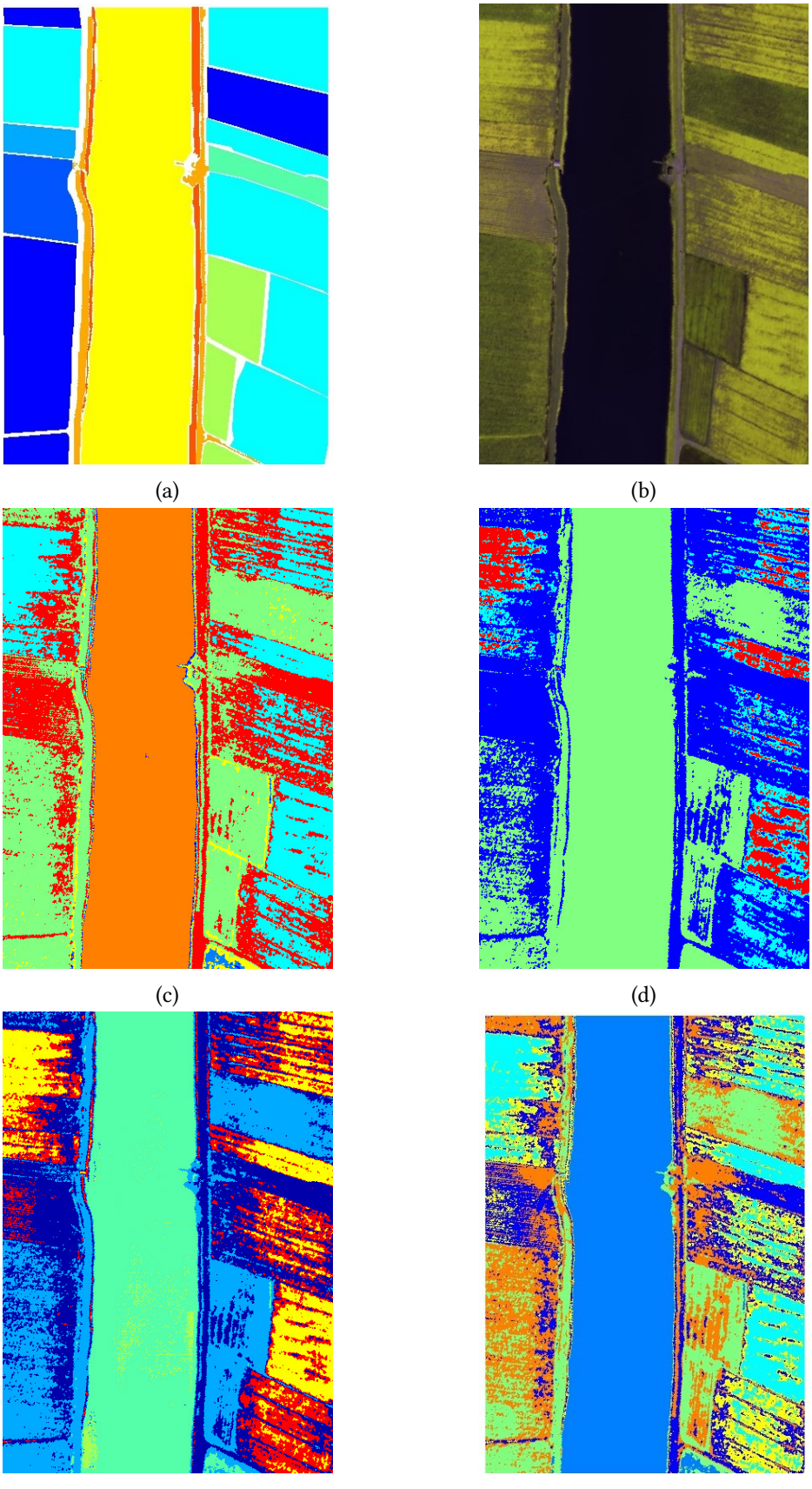

Figure 2: (a) Ground Truth image of WHU Dataset [22] [23], (b) Resultant image using BSSV [11], (c) Clustered image using WaO [8], (d) Clustered image using QbWaO, (e) Clustered image using QtWaO with *AIndex* [13], (f) results using K-means [3] (cluster number = 6) on WHU Dataset [22] [23]

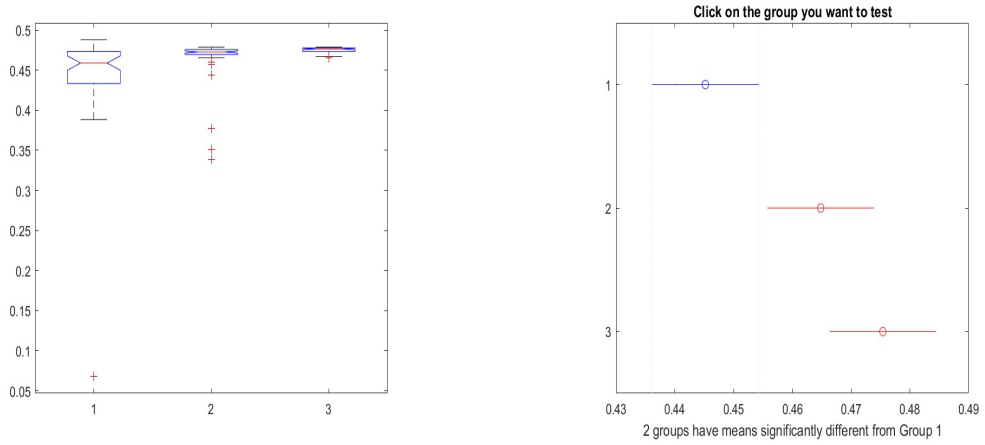

(a) (b)

Figure 3: (a) One-Way ANOVA test [25], (b) Tukey's post hoc test [25] - results for WHU Dataset [22] [23]